Finite element implementation and numerical issues of strain gradient plasticity with application to metal matrix composites

Frederiksson, Per; Gudmundson, Peter; Mikkelsen, Lars Pilgaard

Published in:
International Journal of Solids and Structures

Link to article, DOI:
10.1016/j.ijsolstr.2009.07.028

Publication date:
2009

Document Version
Early version, also known as pre-print

Finite element implementation and numerical issues of strain gradient plasticity with application to metal matrix composites

Per Fredriksson [a,*] Peter Gudmundson [a]
Lars Pilgaard Mikkelsen [b]

[a] *Department of Solid Mechanics, KTH Engineering Sciences, Royal Institute of Technology, Osquars backe 1, SE-100 44 Stockholm, Sweden*

[b] *Materials Research Department, Risø National Laboratory for Sustainable Energy, Technical University of Denmark, DK-4000 Roskilde, Denmark*

Abstract

A framework of finite element equations for strain gradient plasticity is presented. The theoretical framework requires plastic strain degrees of freedom in addition to displacements and a plane strain version is implemented into a commercial finite element code. A couple of different elements of quadrilateral type are examined and a few numerical issues are addressed related to these elements as well as to strain gradient plasticity theories in general. Numerical results are presented for an idealized cell model of a metal matrix composite under shear loading. It is shown that strengthening due to fiber size is captured but strengthening due to fiber shape is not. A few modelling aspects of this problem are discussed as well. An analytic solution is also presented which illustrates similarities to other theories.

Key words: Finite element method, Strain gradient plasticity, Metal matrix composites, Strengthening, Dislocations

* Corresponding author. Tel.: + 46 - (0)10 - 505 44 98 Fax.: + 46 - (0)21 - 12 40 97
Email address: per.fredriksson@afconsult.com (Per Fredriksson).
[1] Present address: ÅF-Infrastruktur AB, Port-Anders Gata 3, SE-722 12 Västerås, Sweden

1 Introduction

The plastic flow of crystalline materials is by nature a multiscale process. Dislocation structures, entanglements and avalanches of dislocations result in strongly heterogeneous plastic deformation in small, confined volumes. Putting together many such small parts of the material, a global irreversible deformation is obtained on the macro scale. One physical motivation for reinforcement of a metal matrix material with fibers, is the obstruction of slip. If a glide path of a dislocation encounter a fiber surface, the dislocation cannot pass the fiber, except for possibly by the Orowan mechanism. In addition, the interface between the elastic fibers and the elastic-plastic matrix material will introduce a constraint on the deformation in the matrix material at the interface and a boundary layer around the fibers will develop. Therefore, smaller fibers will have an increased effect on the flow strength compared to larger fibers at the same fiber volumne fraction, Lloyd (1994). This size-effect in metal matrix composites (MMC) cannot be captured by standard plasticity theories, since no length scale parameters exist in these theories. The enhancement of continuum theories by inserting some length scale parameter into the formulation is a step towards multiscale modelling, see e.g. Aifantis (1987), Fleck and Hutchinson (1997), Gudmundson (2004), Fleck and Willis (2004) who focused on bulk behaviour and Cermelli and Gurtin (2002), Gudmundson and Fredriksson (2003), Aifantis and Willis (2005), Borg and Fleck (2007) who focused on interface models for plastic deformation. Bridging length scales is the strength of strain gradient plasticity theories. They are powerful since the global behaviour is captured through the continuum sense of the theory and the micro processes are modelled in an average sense through higher-order boundary conditions and stresses.

In the present study, we apply the rate-independent strain gradient plasticity framework by Gudmundson (2004). Constitutively, we use the case where the dissipation is independent of the moment stresses. The theory is complemented by the derivation of the incremental stress-strain relations. A general 3D framework of finite element equations of the theory is presented which is used in a 2D analysis of a plane strain model of a fiber reinforced composite under shear loading. Geometrically, the problem is identical to that studied by Bittencourt et al. (2003) and we will discuss similarities as well as differences in the two approaches, see also Cleveringa et al. (1997) and Bassani et al. (2001). In addition, a closed form solution to the one-dimensional pure shear problem is presented, which can be used for comparison to other formulations.

Numerical solution of gradient theories of plasticity by the finite element method has been used in several other studies. One theory that introduces the second gradient of the effective plastic strain measure in the expression for the flow stress is implemented by de Borst and Mühlhaus (1992), see also

Aifantis (1987). The effective plastic strain is by de Borst and Mühlhaus (1992) used in addition to the displacement as nodal degrees of freedom (dof) and higher-order boundary conditions are needed for the same or its conjugate traction. The focus in the theory is directed towards numerical stability for strain softening materials. This can be achieved since ellipticity of the governing differential equations is maintained after entering the softening regime due to the inclusion of the gradient terms in the theory. As a consequence, mesh dependence is avoided after localization, which is demonstrated with 1D numerical results. A drawback of the theory is that C_1-continuity is required for the effective plastic strain field. The same framework has been used by de Borst and Pamin (1996) in a 2D finite element environment. Several 1D and 2D element types, triangles as well as quadrilaterals, are examined numerically. Numerical results of plane strain compression illustrates stability after localization and independence of mesh density as well as mesh direction for the gradient theory. In addition, it is shown that the requirement of C_1-continuity can be avoided through a penalty formulation if the gradients of the effective plastic strain are used as another set of additional dof. Hence three different kinds of dof are used for this penalty formulation. Also, this framework has been used by Mikkelsen (1997) for 2D finite elements. Here, it is shown that the delay of the onset of localization and the post-necking behaviour can be modelled by a plane stress finite element model using the gradient theory, although these are 3D effects. This is accomplished by relating the internal length scale to the current thickness of the thin sheet and the fact that the stress state is essentially two-dimensional. It is also shown that the width of the localized zone is controlled by the internal length scale parameter. Another group of gradient plasticity theories, which introduces the first gradient of plastic strain measures, have also been solved using finite elements. Niordson and Hutchinson (2003) solved plane strain problems by use of the theory presented by Fleck and Hutchinson (2001). The effective plastic strain was required as additional nodal dof and higher-order boundary conditions were needed to be specified for the same or its conjugate traction. Only C_0-continuity was required for the interpolation of the plastic field since no second order gradient enter the formulation. In addition, an implementation in the commercial finite element program Abaqus/Standard 6.7 (2006) has been presented by Mikkelsen (2007). A crystal plasticity version of the gradient dependent plasticity theory was implemented by Borg and Kysar (2007) to analyse the plane strain size-effects of a HCP single crystal. Plastic slips were required as extra dof. Here, 8-noded bi-quadratic quadrilaterals are used for displacements and 4-noded bi-linear quadrilaterals are used for the plastic slip fields. The bi-quadratic Jacobian were used for both fields in order to ensure that the integration points coincided for both fields. The theory in the present paper uses plastic strains in addition to displacements as nodal degrees of freedom. Resulting differential equations are of second order and solution can be obtained using elements of C_0-continuity.

In summary then, the present investigation concerns strain gradient plasticity and it addresses three main topics in particular. First of all, a detailed derivation of both the governing equations and the resulting finite element equations for one paricular choice of constitutive laws (Gudmundson (2004)) is provided and discussed. The finite element equations are given in a matrix formulation which may be useful also for other strain gradient plasticity theories. Secondly, the appearance of several possible finite elements are presented and their numerical behaviour is described and discussed. Perhaps the most distinct feature of this paper is theoretical and numerical issues that arise in 2D- and 3D-frameworks when a combination of a I) a rate-indenpendent formulation is used and II) the plastic part of the strain tensor is used as unknown in addition to the conventional displacements. Several studies have been performed previously in a 1D-context, where many diffuculties are avoided. Or, using a viscoplastic formulation, which can be pushed towards the rate-independent limit, problems that may arise with the definition of a yield surface, yield criterion and consistency relation, are avoided. Secondly, the present implementation is performed using a user element subroutine in Abaqus/Standard 6.7 (2006), which alone is a universal tool for researchers and opens up for a range of possibilities. The problems singled out for analysis are solved and analysed for several reasons. The pure shear problem is more or less a standard problem today and is e.g. ideally suited for comparison between different theoretical formulations. The composite problem is adressed in order to compare to Bittencourt et al. (2003) but also to highlight the physical relevance of the present formulation. Finally, is should be mentioned that the present formulation and implementation has been successfully be used in Fredriksson and Larsson (2008) to simulate the wedge indentation response of thin films on substrates.

2 Formulation

Theoretical frameworks of strain gradient plasticity have been laid down by several authors, including the present ones, that involve one or several length scale parameters. These parameters should be determined in order to properly scale the influence of plastic strain gradients on the material behaviour. The introduction of plastic strain gradients can be done in different ways and this is a step of great challenge in strain gradient plasticity theories. In this section, a theoretical framework will be presented that in our opinion is a quite simple way of introducing plastic strain gradients in a theory that involves enhanced dof and boundary conditions. The formulation was laid down by Gudmundson (2004) and is equally well suited for a rate-independent as well as a rate-dependent constitutive framework. Here, we will use a rate-independent formulation which turns out to have many similarities with conventional von

Mises plasticity. Only the small strain version is introduced.

The fundamental ingredient of the present theory that distinguishes the 'strain gradient' theory from the conventional framework is that plastic strain gradients are considered to contribute to internal work. Consequently, if a free energy per unit volume Ψ of the strain gradient material is to be considered, it should generally be on the form $\Psi = \Psi(\epsilon^{\mathrm{e}}_{ij}, \epsilon^{\mathrm{p}}_{ij}, \epsilon^{\mathrm{p}}_{ij,k})$. The plastic dissipation inequality states that the change of work that is performed within the material $\dot{W}_{\mathrm{i}}$, should always exceed the change in free energy $\dot{\Psi}$, hence

$$\int_V \left(\dot{W}_{\mathrm{i}} - \dot{\Psi}\right) \mathrm{d}V \geq 0 \tag{2.1}$$

If this restriction is assumed to be valid for every volume element, the following equation is obtained

$$\left(\sigma_{ij} - \frac{\partial \Psi}{\partial \epsilon^{\mathrm{e}}_{ij}}\right) \dot{\epsilon}^{\mathrm{e}}_{ij} + \left(q_{ij} - \frac{\partial \Psi}{\partial \epsilon^{\mathrm{p}}_{ij}}\right) \dot{\epsilon}^{\mathrm{p}}_{ij} + \left(m_{ijk} - \frac{\partial \Psi}{\partial \epsilon^{\mathrm{p}}_{ij,k}}\right) \dot{\epsilon}^{\mathrm{p}}_{ij,k} \geq 0 \tag{2.2}$$

or equivalently

$$\bar{\sigma}_{ij} \dot{\epsilon}^{\mathrm{e}}_{ij} + \bar{q}_{ij} \dot{\epsilon}^{\mathrm{p}}_{ij} + \bar{m}_{ijk} \dot{\epsilon}^{\mathrm{p}}_{ij,k} \geq 0. \tag{2.3}$$

Here, we have introduced the conjugate quantities σ_{ij}, q_{ij} and m_{ijk}, which we will refer to as the Cauchy stress, the micro stress and the moment stress, respectively. We can from Eqs. (2.3) and (2.2) conclude that it is the resultant stress measures, denoted with overscript bars $\bar{(\,)}$, that contribute to the dissipation. Two extreme cases can then be defined, one being the energetic case, where all work is stored in Ψ and all stresses can be determined from the free energy. All terms in Eq. (2.3) then vanish. The other one is the dissipative case, which implies that no plastic energy is stored. Hence Ψ does only depend on the elastic strain. Neither of these extreme cases seem to be very realistic (perhaps strictly not even for one stress measure alone for a crystalline material) but a physically motivated model should be somewhere in between. In the present analysis, we will assume the following form of free energy density function

$$\Psi = \frac{1}{2} D_{ijkl} \epsilon^{\mathrm{e}}_{ij} \epsilon^{\mathrm{e}}_{kl} + \Psi_{\mathrm{g}} \tag{2.4}$$

where D_{ijkl} is the tensor of elastic moduli and the last term is attributed to plastic strain gradients

$$\Psi_{\mathrm{g}} = \frac{1}{2} L^2 G \epsilon^{\mathrm{p}}_{ij,k} \epsilon^{\mathrm{p}}_{ij,k} \tag{2.5}$$

The parameter L is an energetic length scale parameter and G is the shear modulus. The first term of the free energy arises due to elastic work, which is conventional. The last term is included due to plastic strain gradients based on the influence from geometrically necessary dislocations. Here, an alternative formulation could introduce the Nye dislocation tensor in Ψ_{g}, which has a more direct connection to geometrically necessary dislocations. We also stress the importance of differentiating between an energetic length scale and a dissipative one, such as the one introduced in the formulation by Fredriksson and Gudmundson (2007). This difference has also been emphasized by Anand et al. (2005).

In the following, we will assume that both the Cauchy stress and the moment stress is purely energetic. Consequently, $\bar{\sigma}_{ij} = 0, \bar{m}_{ijk} = 0$, which means that all work that is associated with them is stored and the following relations are found

$$\sigma_{ij} = \frac{\partial \Psi}{\partial \epsilon^{\mathrm{e}}_{ij}} = D_{ijkl} \epsilon^{\mathrm{e}}_{kl} \tag{2.6}$$

$$q_{ij} = \bar{q}_{ij} \tag{2.7}$$

$$m_{ijk} = \frac{\partial \Psi}{\partial \epsilon^{\mathrm{p}}_{ij,k}} = G L^2 \epsilon^{\mathrm{p}}_{ij,k} \tag{2.8}$$

As a consequence of (2.4), the dissipation per unit volume (2.2) can be simplified to

$$q_{ij} \dot{\epsilon}^{\mathrm{p}}_{ij} \geq 0. \tag{2.9}$$

This expression is very similar to the plastic dissipation in conventional plasticity. The very important difference is though, that the role played by the stress deviator in conventional plasticity is here played by the micro stress. Note also, that the micro stress is by nature deviatoric, hence the hydrostatic part never enters the theory.

We assume the existence of a flow surface f, such that

$$f = q_{\mathrm{e}} - \sigma_{\mathrm{f}} = 0 \tag{2.10}$$

is required for plastic loading. An effective micro stress q_{e} and a flow stress σ_{f} have been introduced. At this point, we will only pay attention to linear, isotropic hardening $\sigma_{\mathrm{f}} = \sigma_{\mathrm{y}} + H\epsilon_{\mathrm{e}}^{\mathrm{p}}$, where σ_{y} is the yield stress, H is a hardening modulus and $\epsilon_{\mathrm{e}}^{\mathrm{p}}$ is an effective plastic strain. Since the moment stress does not enter in Eq. (2.9), the effective stress is composed as a quadratic form in q_{ij} only:

$$q_{\mathrm{e}} = \sqrt{\frac{3}{2} q_{ij} q_{ij}} \tag{2.11}$$

Provided Eq. (2.10) is fulfilled, it is assumed that the plastic strain increment direction is determined by the normal to the flow surface

$$\dot{\epsilon}_{ij}^{\mathrm{p}} = \dot{\lambda} \frac{\partial f}{\partial q_{ij}} = \dot{\lambda} \frac{3}{2} \frac{q_{ij}}{q_{\mathrm{e}}} \tag{2.12}$$

where $\dot{\lambda}$ is a plastic multiplier. Multiplying (2.12) by itself yields the identification $\dot{\lambda} = \dot{\epsilon}_{\mathrm{e}}^{\mathrm{p}} = \sqrt{2/3\ \dot{\epsilon}_{ij}^{\mathrm{p}} \dot{\epsilon}_{ij}^{\mathrm{p}}}$. In order to ensure that the stress state does not leave the flow surface, a consistency relation has to be fulfilled:

$$\dot{f} = \frac{\partial q_{\mathrm{e}}}{\partial q_{ij}} \dot{q}_{ij} - H\dot{\lambda} = 0 \tag{2.13}$$

where $H = \mathrm{d}\sigma_{\mathrm{f}} / \mathrm{d}\epsilon_{\mathrm{e}}^{\mathrm{p}}$.

2.1 Tangent stiffnesses

In conventional plasticity theory, the tangent stiffness matrix defines the relation between the stress increments and the total strain increments. In the present theory, such a relation is not possible to find since the plastic part of the strain tensor is used as an independent variable together with displacement. The consistency relation (2.13) then give relations for the micro stress,

not the Cauchy stress. Instead, relations for $\dot{q}_{ij}$ is sought for in terms of $\dot{\epsilon}^{\mathrm{p}}_{ij}$. If we let $r_{ij} = \frac{3}{2}\frac{q_{ij}}{q_{\mathrm{e}}}$, which is a tensor governing the direction of plastic flow, we have

$$\dot{q}_{ij} = \dot{\overline{\frac{2}{3} q_{\mathrm{e}} r_{ij}}} = \frac{2}{3}(\dot{q}_{\mathrm{e}} r_{ij} + q_{\mathrm{e}} \dot{r}_{ij}) \tag{2.14}$$

Then with

$$\dot{q}_{\mathrm{e}} = H\dot{\lambda} \tag{2.15}$$

$$\dot{\lambda} = \frac{2}{3} r_{ij} \dot{\epsilon}^{\mathrm{p}}_{ij} \tag{2.16}$$

we get

$$\dot{q}_{ij} = \frac{2}{3}\left[\frac{2}{3} H r_{ij} r_{kl} \dot{\epsilon}^{\mathrm{p}}_{kl} + \underbrace{q_{\mathrm{e}} \dot{r}_{ij}}_{\dot{q}^{\mathrm{c}}_{ij}}\right] \tag{2.17}$$

The term $\dot{q}^{\mathrm{c}}_{ij}$ is unknown and does not coincide with the direction of plastic flow. In order to fulfill normality, we want the plastic strain increment to be perpendicular to the flow surface. This is accomplished by imposing the constraint

$$\dot{\epsilon}^{\mathrm{pc}}_{ij} = \dot{\epsilon}^{\mathrm{p}}_{ij} - \frac{2}{3} r_{ij} r_{kl} \dot{\epsilon}^{\mathrm{p}}_{kl} = 0, \tag{2.18}$$

which means that the increment in plastic strain tangential to the flow surface should vanish. One way to fulfill this requirement is by assuming

$$\dot{q}^{\mathrm{c}}_{ij} = E_0 \dot{\epsilon}^{\mathrm{pc}}_{ij} \tag{2.19}$$

where E_0 is a penalty parameter. Eq. (2.18) is then fulfilled identically if $E_0 \to \infty$ but should in numerical calculations be set to a value that is sufficiently large to yield an acceptable solution. The resulting expression then is

$$\dot{q}_{ij} = \frac{2}{3}\left[\frac{2}{3}(H - E_0) r_{ij} r_{kl} \dot{\epsilon}^{\mathrm{p}}_{kl} + E_0 \dot{\epsilon}^{\mathrm{p}}_{ij}\right] \tag{2.20}$$

The increment of moment stress m_{ijk} is simply found to be

$$\dot{m}_{ijk} = GL^2 \dot{\epsilon}^{\mathrm{p}}_{ij,k} \tag{2.21}$$

In summary, all the stress quantities can be updated with the following set of equations:

$$\dot{\sigma}_{ij} = D_{ijkl}(\dot{\epsilon}_{kl} - \dot{\epsilon}^{\mathrm{p}}_{kl}) \tag{2.22}$$

$$\dot{q}_{ij} = \frac{2}{3}\left[\frac{2}{3}(H - E_0) r_{ij} r_{kl} + E_0 \delta_{ik}\delta_{jl}\right] \dot{\epsilon}^{\mathrm{p}}_{kl} \tag{2.23}$$

$$\dot{m}_{ijk} = GL^2 \dot{\epsilon}^{\mathrm{p}}_{ij,k} \tag{2.24}$$

where δ_{mn} is the Kronecker delta function and $r_{ij} = \frac{3}{2}\frac{q_{ij}}{q_{\mathrm{e}}}$. All the variables on the right hand side may then be obtained from either $\dot{u}_i$ or $\dot{\epsilon}^{\mathrm{p}}_{ij}$. It should be noted that q_{ii} and $m_{ii,k}$ never enter the formulation.

2.2 Variational principle and finite element equations

A finite element implementation of the above framework has been based on the principle of virtual work. An enhanced version of the incremental variational principle presented in Gudmundson (2004) is applied

$$\begin{aligned}\int_V \left(\dot{\sigma}_{ij}\delta\dot{\epsilon}_{ij} + (\dot{q}_{ij} - \dot{\sigma}_{ij})\delta\dot{\epsilon}^{\mathrm{p}}_{ij} + \dot{m}_{ijk}\delta\dot{\epsilon}^{\mathrm{p}}_{ij,k}\right) \mathrm{d}V\Big|_{t=t_{n+1}} &= \int_S (\dot{T}_i \delta\dot{u}_i + \dot{M}_{ij}\delta\dot{\epsilon}^{\mathrm{p}}_{ij})\mathrm{d}S\Big|_{t=t_{n+1}} \\ - \left\{\int_V \left(\sigma_{ij}\delta\dot{\epsilon}_{ij} + (q_{ij} - \sigma_{ij})\delta\dot{\epsilon}^{\mathrm{p}}_{ij} + m_{ijk}\delta\dot{\epsilon}^{\mathrm{p}}_{ij,k}\right) \mathrm{d}V - \int_S (T_i\delta\dot{u}_i + M_{ij}\delta\dot{\epsilon}^{\mathrm{p}}_{ij})\mathrm{d}S\right\}_{t=t_n}\end{aligned} \tag{2.25}$$

where the bracket terms are equilibrium correction terms evaluated at the time $t = t_n$. The corresponding strong form is the two sets of differential equations

$$\sigma_{ij,j} = 0 \qquad \text{in } V \tag{2.26}$$

$$m_{ijk,k} + s_{ij} - q_{ij} = 0 \qquad \text{in } V, \tag{2.27}$$

which have to be fulfilled together with boundary conditions for $\dot{u}_i$ and $\dot{\epsilon}^{\mathrm{p}}_{ij}$ or $\dot{T}_i = \dot{\sigma}_{ij} n_j$ and $\dot{M}_{ij} = \dot{m}_{ijk} n_k$, respectively. Eq. (2.26) is the conventional equilibrium equation in the absence of body forces and Eq. (2.27) balances the higher-order stresses according to the amount of gradient effects. In the absence of any gradients in plastic strain, Eq. (2.27) is redundant, since m_{ijk} then vanishes and $q_{ij} = s_{ij}$ results.

For numerical solution by the finite element method, a discretization technique is used that employs not only the displacements u_i, but also the plastic strains $\epsilon^{\mathrm{p}}_{ij}$ as independent variables:

$$u_i = \sum_{I=1}^{n_{\mathrm{u}}} N^I_{\mathrm{u}}(\xi_k) d^I_i \tag{2.28}$$

$$\epsilon^{\mathrm{p}}_{ij} = \sum_{I=1}^{n_{\mathrm{p}}} N^I_{\mathrm{p}}(\xi_k) e^I_{ij} \tag{2.29}$$

Here, ξ_i denotes three natural coordinates, e^I_{ij} and d^I_i are nodal values at node I for plastic strains and displacements, respectively and N^I_{p} and N^I_{u} are shape functions. The number of nodes used are n_{u} and n_{p} for the displacement field and plastic strain field, respectively. Strains and plastic strain gradients are obtained as the derivatives

$$\epsilon_{ij} = \sum_{I=1}^{n_{\mathrm{u}}} \frac{1}{2} \left(B^I_{\mathrm{u}j} d^I_i + B^I_{\mathrm{u}i} d^I_j \right) \tag{2.30}$$

$$\epsilon^{\mathrm{p}}_{ij,k} = \sum_{I=1}^{n_{\mathrm{p}}} B^I_{\mathrm{p}k} e^I_{ij} \tag{2.31}$$

where $B^I_{\mathrm{u}i}$ and $B^I_{\mathrm{p}i}$ are spatial derivatives of the shape functions for displacements and plastic strains, respectively. Eq. (2.25) can now be written in matrix form (see Appendix A for details)

$$\mathbf{k}_{\mathrm{e}} \dot{\mathbf{p}}^{n+1}_{\mathrm{e}} = \dot{\mathbf{f}}^{n+1}_{\mathrm{e}} - \{\mathbf{c}^n_{\mathrm{i}} - \mathbf{c}^n_{\mathrm{e}}\} \tag{2.32}$$

where

$$\mathbf{k}_{\mathrm{e}} = \begin{bmatrix} \mathbf{k}_{\mathrm{u}} & -\mathbf{k}_{\mathrm{up}} \\ -\mathbf{k}^{\mathrm{T}}_{\mathrm{up}} & \mathbf{k}_{\mathrm{p}} \end{bmatrix}, \quad \dot{\mathbf{f}}_{\mathrm{e}} = \int_S \begin{bmatrix} \mathbf{N}^{\mathrm{T}}_{\mathrm{u}} \dot{\mathbf{t}}_{\mathrm{u}} \\ \mathbf{N}^{\mathrm{T}}_{\mathrm{p}} \dot{\mathbf{t}}_{\mathrm{p}} \end{bmatrix} \mathrm{d}S \tag{2.33}$$

is the element stiffness matrix and force vector, respectively. The bracket terms, which read

$$\mathbf{c}_{\mathrm{i}} = \int_S \mathbf{B}^{\mathrm{T}} \mathbf{s} \mathrm{d}V, \quad \mathbf{c}_{\mathrm{e}} = \int_S \mathbf{N}^{\mathrm{T}} \mathbf{t} \mathrm{d}S \tag{2.34}$$

are equilibrium correction terms and $\dot{\mathbf{p}}_{\mathrm{e}}^{\mathrm{T}} = \left[\dot{\mathbf{d}}^{\mathrm{T}} \ \dot{\mathbf{e}}^{\mathrm{T}} \right]$ is a vector of displacement and plastic strain dof, respectively. Explicitly, we have

$$\mathbf{k}_{\mathrm{u}} = \int_V \mathbf{B}_{\mathrm{u}}^{\mathrm{T}} \mathbf{D} \mathbf{B}_{\mathrm{u}} \ \mathrm{d}V \tag{2.35}$$

$$\mathbf{k}_{\mathrm{up}} = \int_V \mathbf{B}_{\mathrm{u}}^{\mathrm{T}} \mathbf{D} \mathbf{N}_{\mathrm{p}} \ \mathrm{d}V \tag{2.36}$$

$$\mathbf{k}_{\mathrm{p}} = \int_V \left[\mathbf{N}_{\mathrm{p}}^{\mathrm{T}} (\mathbf{D}_{\mathrm{q}} + \mathbf{D}) \mathbf{N}_{\mathrm{p}} + \mathbf{B}_{\mathrm{p}}^{\mathrm{T}} \mathbf{D}_{\mathrm{m}} \mathbf{B}_{\mathrm{p}} \right] \ \mathrm{d}V \tag{2.37}$$

where

$$\mathbf{D}_{\mathrm{q}} = \frac{2}{3} \left[\frac{2}{3} (H - E_0) \mathbf{r}\mathbf{r}^{\mathrm{T}} + E_0 \mathbf{I}_{\mathrm{q}} \right] \tag{2.38}$$

$$\mathbf{I}_{\mathrm{q}} = \mathrm{diag} \left[\begin{array}{cccccc} 1 & 1 & 1 & 1/2 & 1/2 & 1/2 \end{array} \right] \tag{2.39}$$

$$\mathbf{D}_{\mathrm{m}} = GL^2 \mathbf{I}_{\mathrm{m}} \tag{2.40}$$

$$\mathbf{I}_{\mathrm{m}} = \left[\begin{array}{ccc} \mathbf{I}_{\mathrm{q}} & \mathbf{0} & \mathbf{0} \\ \mathbf{0} & \mathbf{I}_{\mathrm{q}} & \mathbf{0} \\ \mathbf{0} & \mathbf{0} & \mathbf{I}_{\mathrm{q}} \end{array} \right] \tag{2.41}$$

and $[\mathbf{r}]_{ij} = \frac{3}{2} \frac{q_{ij}}{q_{\mathrm{e}}}$, $\mathbf{D}$ is the elasticity matrix and $\mathbf{0}$ is the zero matrix. Eq. (2.32) is the governing equation for one element.

A plane strain version of this framework has been implemented in the general purpose finite element code Abaqus/Standard 6.7 (2006) in terms of the user subroutine UEL, which is a general element formulation provided by the user. Both geometrically linear and quadratic elements have been examined. All shape functions are standard first and second order polynomials used for conventional 2D solid elements. In the 2D version, two dof at each node (d_1^I, d_2^I) are used for the displacements (u_1, u_2) and three dof $(e_{11}^I, e_{22}^I, e_{12}^I)$ are used for the plastic strains $(\epsilon_{11}^{\mathrm{p}}, \epsilon_{22}^{\mathrm{p}}, \epsilon_{12}^{\mathrm{p}})$. Generally, in a plane strain situation, the plastic part of the out-of-plane strain, here $\epsilon_{33}^{\mathrm{p}}$, does not vanish. It is however constrained due to the assumption of plastic incompressibility, see the Appendix for details on how this is treated.

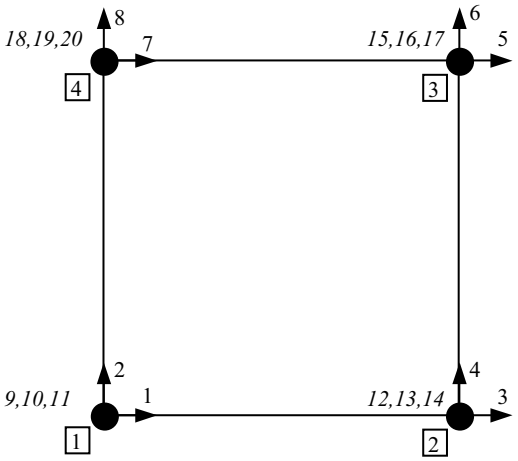

(a) 4-noded bi-linear element with the number of displacement dof $2n_{\mathrm{u}} = 8$ and plastic strain dof $3n_{\mathrm{p}} = 12$, i.e. displacement and plastic strain fields use 4 nodes, 20 dof in total; labels are **4F** for full integration and **4R** for reduced integration, respectively.

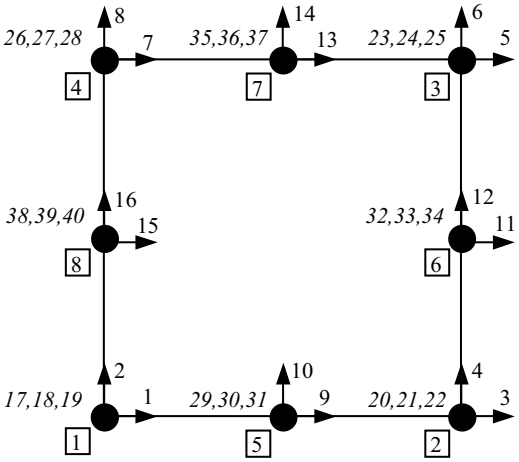

(b) 8-noded bi-quadratic element with $2n_{\mathrm{u}} = 16$ and $3n_{\mathrm{p}} = 24$, i.e. 5 dof at all nodes, 40 dof in total. Labels used are **8F** and **8R**.

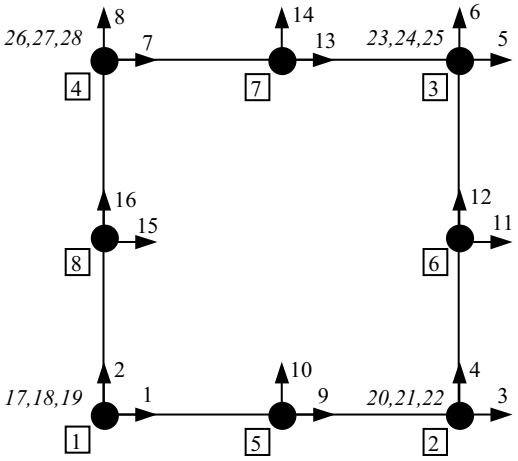

(c) 8-noded combined bi-quadratic element with $2n_{\mathrm{u}} = 16$ and $3n_{\mathrm{p}} = 12$, i.e. all nodes are used for the displacement field and only corner nodes are used for the plastic strain field. The geometrical mapping is quadratic, 28 dof in total; labels are **8CF** and **8CR**, respectively.

Fig. 1. Different element types examined. The numbering of plastic strain dof is in italic and displacement dof in normal font.

Numerical integration is performed in a forward Euler manner, with a large number of small time increments. Depending on whether a point is considered as elastic or plastic, the integration of Eqs. (2.33, 2.34) is done in a non-

standard manner. If the point is elastic, $\mathbf{k}_{\text{up}} = \mathbf{0}$ and $\mathbf{k}_{\text{p}} = 10^8 E\mathbf{I}$, where E is Young's modulus and $\mathbf{I}$ is the identity matrix. In this way, $\dot{\mathbf{e}} = \mathbf{0}$ is obtained and no plastic increments results. Stress update is performed according to $\dot{q}_{ij} = \dot{s}_{ij}$ and $\dot{m}_{ijk} = 0$. If a point is plastic, $\mathbf{k}_{\text{e}}$ is a full matrix and both displacement and plastic strain increments are obtained when Eq. (2.32) is solved. Update follows Eqs. (2.22-2.24).

During the course of the implementation, three different kinds of elements of quadrilateral type have been analysed, see Fig. 1. Two of them have five dof per node, one 8-noded bi-quadratic element and one 4-noded bi-linear element. The third type is an 8-noded element which is bi-quadratic in displacement, where the plastic strain field only utilizes the corner nodes. The geometrical mapping is however quadratic, which means that the same Jacobian is always used for both fields. In the following, we will use labels when referring to the different element types. c.f. Fig. 1. The number in the label denotes the number of nodes of the element and the letter denotes either full or reduced integration. If there is a C in the label, the combined 8-4-noded element is intended, hence **8CR** means the combined 8-4-noded element using reduced integration.

3 Results

3.1 Analytic solution to the simplest problem

In this section, pure shear of a thin film will be solved analytically. The film occupies the $xy-$plane, has thickness h and is large in the y-direction such that the only spatial dependence will be on the x-coordinate. The only strain component is the shear strain $\gamma = 2\epsilon_{xy} = 2\epsilon_{yx}$ and the shear stress is $\tau = \sigma_{xy} = \sigma_{yx}$. Based on the same arguments, the only non-vanishing micro and moment stresses are $q = q_{xy} = q_{yx}$ and $m = m_{xyy} = m_{yxy}$, respectively. The loading consists of a shearing displacement of the top surface $u = u_x = h\Gamma$, while the bottom surface is held fixed. The boundary conditions are

$$\gamma_{\text{p}} = 0 \qquad \text{at} \quad x = 0, h \tag{3.1}$$

$$u = 0 \qquad \text{at} \quad x = 0 \tag{3.2}$$

Equation (3.1) can be physically motivated if the film surfaces are attached to some other material which will act as a plastic constraint at the film interfaces, since the dislocations are not allowed to leave the surface. The two primary variables are the displacement u and the plastic shear strain γ_{p}. If monotonic loading is assumed, $\dot{\Gamma} > 0$, the effective plastic strain may be integrated to

$\epsilon_{\mathrm{e}}^{\mathrm{p}} = \int \dot{\epsilon}_{\mathrm{e}}^{\mathrm{p}} \mathrm{d}t = \gamma_{\mathrm{p}}/\sqrt{3}$. The yield condition Eq. (2.10) then gives a relation between the micro stress and the plastic shear $q = \sigma_{\mathrm{y}}/\sqrt{3} + (H/3)\ \gamma_{\mathrm{p}}$. The moment stress is directly given by the free energy from Eq. (2.8) as $m = GL^2 \frac{\mathrm{d}\gamma_{\mathrm{p}}}{\mathrm{d}x}$. Using the sets (2.26) and (2.27), the problem can then be formulated as two second-order, linear, differential equations for the displacement and the plastic shear:

$$\frac{\mathrm{d}^2 u}{\mathrm{d}x^2} - \frac{\mathrm{d}\gamma_{\mathrm{p}}}{\mathrm{d}x} = 0 \tag{3.3}$$

$$\frac{\mathrm{d}^2 \gamma_{\mathrm{p}}}{\mathrm{d}x^2} - \frac{3G + H}{3GL^2}\gamma_{\mathrm{p}} + \frac{1}{L^2}\frac{\mathrm{d}u}{\mathrm{d}x} = \frac{\sigma_{\mathrm{y}}}{\sqrt{3}GL^2} \tag{3.4}$$

Knowing that the shear stress is spatially constant due to equilibrium, Eq. (3.4) can be rewritten as

$$\frac{\mathrm{d}^2 \gamma_{\mathrm{p}}}{\mathrm{d}x^2} - \alpha\gamma_{\mathrm{p}} = -T \tag{3.5}$$

where

$$\alpha = \frac{H}{3GL^2} > 0 \tag{3.6}$$

$$T = \frac{\tau - \sigma_{\mathrm{y}}/\sqrt{3}}{GL^2} > 0 \tag{3.7}$$

The solution to Eq. (3.5) with boundary conditions Eq. (3.1) is given by

$$\gamma_{\mathrm{p}} = \frac{T}{\alpha}\left[-\cosh\sqrt{\alpha}x + \frac{\cosh\sqrt{\alpha}h - 1}{\sinh\sqrt{\alpha}h}\sinh\sqrt{\alpha}x + 1\right] \tag{3.8}$$

It can be noted that the functional form is the same as the solution with the theory by Gurtin (2002) [2]. The resulting shear stress for a given average shear strain Γ can then be obtained from Hooke's law Eq. (2.6) for τ with Γ prescribed. In Fig. 2, the analytic solution is shown together with results predicted by the finite element implementation of the theory for different values of the length parameter L.

[2] Conventional plasticity theory would predict γ_{p} spatially constant, since Eq. (3.1) is not covered by that theory. The same prediction would be obtained by a so-called lower-order strain gradient plasticity theory, since no plastic strain gradient can be

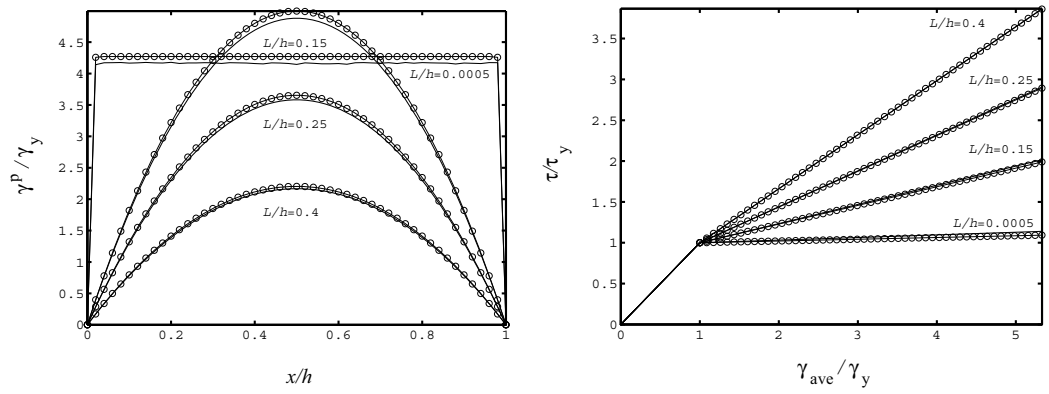

(a) (b)

Fig. 2. Results for pure shear, analytic (solid line with circles) as well as finite element (solid line) results for different values of the length scale parameter. (a) Distribution of plastic shear strain through the thickness of the film at $\Gamma = 0.02$. (b) Shear stress vs. average shear strain relations.

In Fig. 2(a), the plastic shear strain distribution at $\Gamma = 0.02$ is shown and in Fig. 2(b), shear stress vs. average shear strain is shown. The finite element results are generated with element type **8CR** and it can be seen that the finite element results follows the analytic solution. Comments on numerics can be found in Section 3.3.

3.2 Metal matrix composite

A metal reinforced with fibers is analysed numerically. The size-effect of small fibers giving more strengthening compared to large fibers for the same volume fraction of fibers (Lloyd (1994)), cannot be captured with conventional plasticity theory. In the present study, the matrix material of the metal matrix composite (MMC) is assumed to deform elastic-plastically and is modelled with the present gradient theory, while the fibers are assumed to remain elastic. The problem has been studied by several authors previously, of which the current geometrical setup, see Fig. 3, is identical to the one by Bittencourt et al. (2003) and we will later on discuss some issues compared to that study. The fiber distribution can be described with two periodic arrays of equally sized fibers. A unit cell of the material then consists of one quarter of a fiber in each corner surrounding one fiber in the middle. The cell is a plane strain model of a cross section of a specimen of the material. The cell has dimensions $2w \times 2h$, with $w = \sqrt{3}h$ and the fibers $2w_{\rm f} \times 2h_{\rm f}$. Two fiber configurations, both with fiber volume fraction 0.2 are studied. Configuration A is one having more rectangular fibers and B is one having fibers with a quadratic cross-section, see Fig. 3. On purely geometrical arguments, for certain special cases of mi-

triggered in the absence of Eq. (3.1).

crostructures, the case B would offer a possibility for slip bands to develop where plastic slip could localize without any fiber interference, but in the case A that would not be possible.

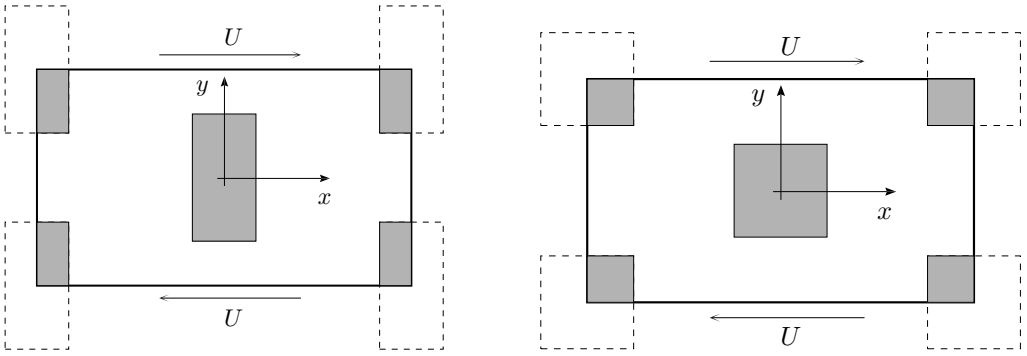

(a) (b)

Fig. 3. Unit cell model of the metal matrix composite. Two fiber configurations are studied, both with the fiber volume fraction 0.2: (a) configuration A, $h_\mathrm{f} = 2w_\mathrm{f} = 0.588h$ and (b) configuration B, $h_\mathrm{f} = w_\mathrm{f} = 0.416h$.

The loading consists of the shearing displacement

$$\begin{aligned} u_x &= \quad h\Gamma \quad \text{at} \quad y = h \\ u_x &= -h\Gamma \quad \text{at} \quad y = -h \\ u_y &= \quad 0 \quad \text{at} \quad x = w, -w \end{aligned} \tag{3.9}$$

The parameter Γ is then the global average shear strain of the unit cell. Higher-order boundary conditions are assumed to be governed by the following mechanism: At the fiber-matrix interfaces, dislocation movement is constrained because of the interface surface to the elastically deforming fibers. If dislocations are present but immobile, plastic deformation cannot develop. Therefore, the plastic strain is forced to vanish at the interfaces. On the outer boundaries of the unit cell, the plastic strain gradient has to vanish due to symmetry. This corresponds to a vanishing moment traction:

$$\begin{aligned} \epsilon^\mathrm{p}_{ij} &= 0 \quad \text{at all fiber}-\text{matrix interfaces} \\ M_{ij} &= 0 \quad \text{at } x = w, -w \text{ and } y = h, -h \end{aligned} \tag{3.10}$$

In the calculations, the following parameters have been used: $E = 40H$, $\sigma_\mathrm{y} = H/10$, $\nu = 0.3$ and $E_0 = 100H$ and results are generated with the element type **4F**. The force-displacement relationship for the two fiber configurations are shown together with the conventional J_2-solution in Fig. 4. It can be

seen that there are virtually no difference between the predictions by the present gradient theory for fiber configurations A or B. A strong size-effect exist however for smaller fibers at constant volume fraction, which is illustrated by a varying ratio L/h.

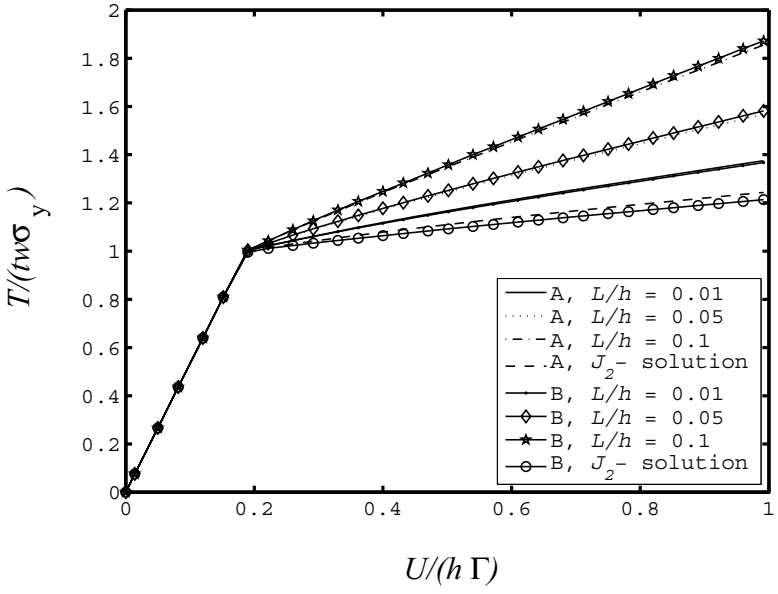

Fig. 4. Normalized relations for average shear force vs. displacement for both fiber configurations A and B at $\Gamma = 0.02$. The relations are shown for different ratios between internal length scale L and dimension parameter h. The solution for conventional J_2-plasticity theory is included.

The distribution of plastic shear strain is shown in Figs. (5,6,7,8) at an average shear of $\Gamma = 0.02$. It can be seen that, compared to the J_2-solution in Figs. (5,7), the gradient theory solutions reduce the amount of plastic deformation throughout the whole metal matrix composite, with a higher plastic constraint for a higher internal length scale parameter L. Also, plastic strain gradients are suppressed, leading to a smoother plastic strain field. For both A and B, the areas of maximum plastic shear are located far away from the fibers due to the boundary condition on plastic shear. This behaviour seems intuitively physically correct for small fibers, i.e. a high ratio L/h. Strong boundary layers may then develop due to reduced dislocation movement that suppress plastic deformation, which also is predicted in the simulations. It can clearly be seen that plasticity does not localize in the case B, although it is geometrically possible. Note the different contour levels in the figures.

There is a major difference between the present assumptions and the ones by Bittencourt et al. (2003). In the present paper, the plastic behaviour of the metal matrix is assumed to be isotropic. This is true if the number of grains in the unit cell is sufficient in order to average the behaviour and the orientation of the grains are close to random. In Bittencourt et al. (2003), a crystal plasticity framework was used with one active slip system in the

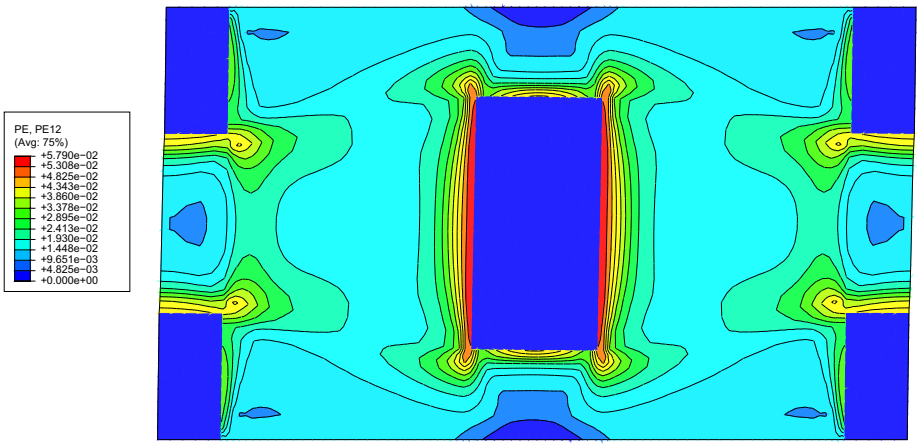

Fig. 5. Contours of plastic shear strain for fiber configuration A at $\Gamma = 0.02$ when the matrix is described by conventional J_2-plasticity theory.

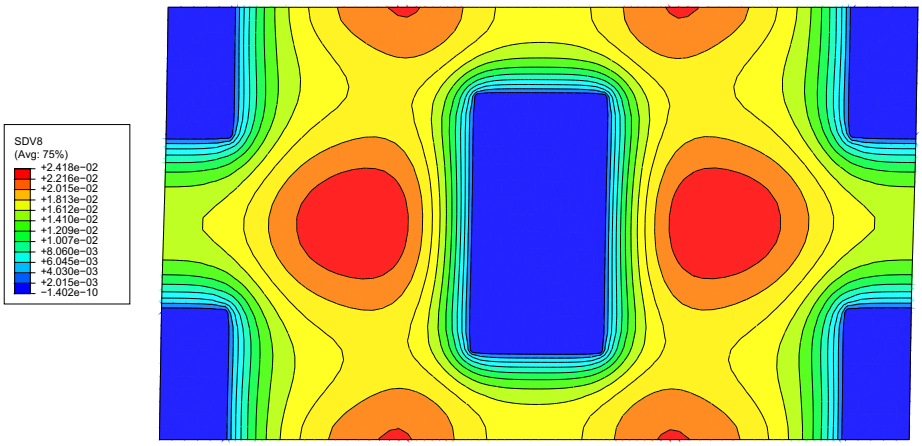

Fig. 6. Contours of plastic shear strain for fiber configuration A at $\Gamma = 0.02$ when the matrix is described by $L/h = 0.1$.

shear direction. Such a situation is relevant either if the MMC is a single crystal, such that the fibers are contained in one single grain which is oriented for slip in the shearing direction, or if it is a polycrystal with unidirectional grains. The grains have to be oriented such that slip is activated simultaneously throughout all of them. These properties are fundamental to the predicted behaviour of the composite. In the case B, it is possible to slice the unit cell

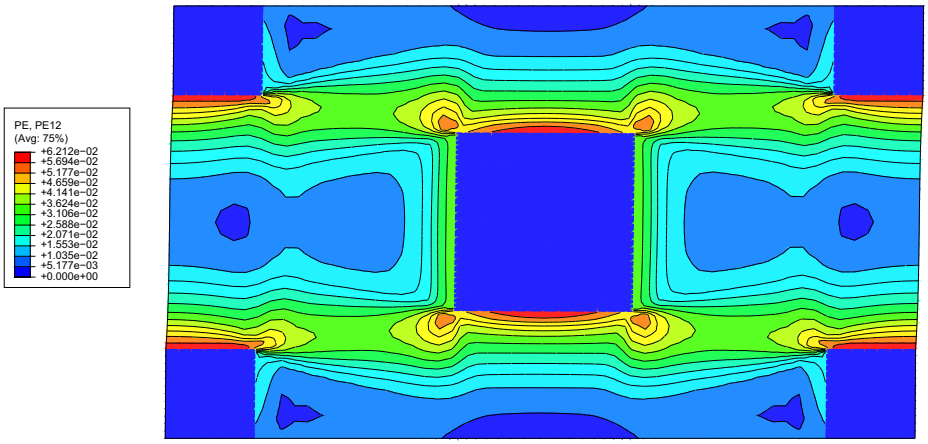

Fig. 7. Contours of plastic shear strain for fiber configuration B at $\Gamma = 0.02$ when the matrix is described by conventional J_2-plasticity theory.

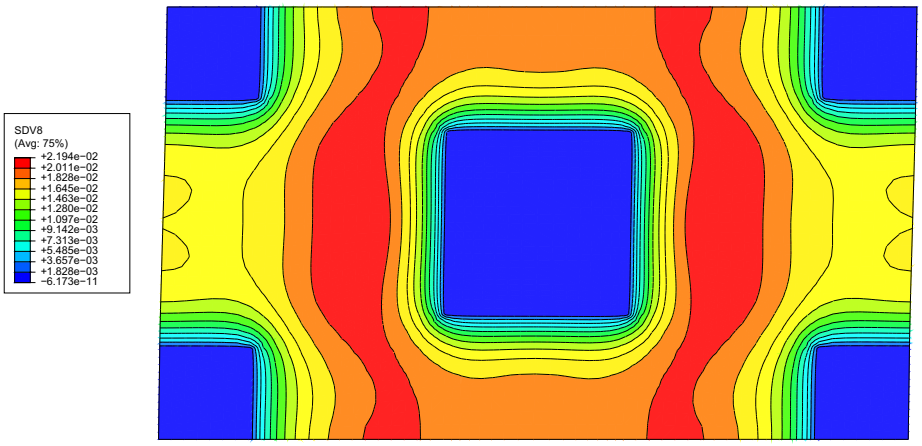

Fig. 8. Contours of plastic shear strain for fiber configuration B at $\Gamma = 0.02$ when the matrix is described by $L/h = 0.1$.

in the x-direction without hitting any fiber. The MMC is then fiber reinforced but have unreinforced veins. In a crystal plasticity framework, plastic slip is then possible on these unreinforced veins without any fiber interference. Hence, plastic deformation may localize to these regions and no contribution to hardening is obtained from the fibers on these planes. This was found by Bittencourt et al. (2003) for both DD simulations and continuum crystal

plasticity with single slip. In an isotropic framework, the deformation cannot be localized in this way.

3.3 Numerical issues

The element types in Fig. 1 have been examined in the search for a possible recommendation on which type should be used in the present theoretical framework. All elements have been tested and are compatible with all pure stress states associated with the plane strain situation. Some numerical observations have been made and are described below. For the pure shear problem, which is a 1D problem and therefore can be solved using only one column of 2D quadrilateral elements, the element types show similar behaviour. At the boundary layer that develops due to the higher-order boundary condition Eq. (3.1), stress oscillations have been found. These are very local and does not affect the global stress-strain response. For the **8CR** element, these oscillations disappear. Furthermore, small values of the length scale parameter imply very large gradients at the boundaries and requires a fine element mesh as well as many time steps in order to yield an accurate solution. In addition, oscillations in the plastic part of the solution have been observed and enhanced numerical methods are suggested to resolve this issue. For the **4R** element, local peaks in the plastic shear strain distribution have been found, possibly related to spurious modes. With the present set of degrees of freedom, spurious modes can generally appear on either the displacement field or the plastic strain field. For the latter, it would however not result in mesh instability, but rather oscillations in the field variables. In the composite problem, all element types have an overall good performance. With the **8F** element, small, local deviations from the behaviour of other elements have been observed on the stress field. This can be seen as a zig-zag pattern in the contour plots. The performance of the **4R** element is better in the composite problem than the pure shear problem, despite the absence of hourglass control. The present setup has a high degree of constraint, both concerning boundary conditions on displacement and plastic strain, and compatible hourglass modes are likely to appear in a more unconstrained environment. Independent of the type of problem studied, points in the plastic regime have been observed drifting at the yield surface such that the point occasionally falls inside the yield surface. An elastic increment then follows, after which plastic loading continues. The effect of this behaviour fades away as the number of time steps is increased. As a remedy, enhanced numerical methods are suggested, which also is of interest for future work. Based on the observations above, the ambition to minimize computational time and the space of storage, the **4F** element has been the default element, and **8CR** is the second choice. The **4R** element should be used with caution. It is emphasized that no preferable choice is known to the author, but a judgment has to be made for each problem setup. For other strain

gradient plasticity theories, the theoretical frameworks can be fundamentally different and tests have to be performed in each individual case.

4 Discussion

The need for a penalty parameter in the constitutive description originates from the consistent connection between plastic strain and micro stress. Some alternative formulations in the literature relate plastic strain to the stress deviator in the same way as conventional theory, although higher-order stresses are introduced. It is believed that since the dissipation is controlled by the micro stress, so should the direction of plastic flow. This requirement is believed to be inherent, since the purpose of the model is to capture size-effects in the plastic regime only. As a consequence, additional work by *plastic* strain gradients are included in the internal virtual work. For theories that introduce the *total* strain gradient (second gradient of displacement) in the internal work expression, the need for a penalty parameter in the constitutive description is avoided. However, in that case the strain gradient will also affect the *elastic* behaviour, leading to an elastic size-effect, which is not consistent with experimental results.

The purpose of the constraint Eq. (2.18) is to ensure a plastic increment perpendicular to the flow surface. This is solved by the penalty method in Eq. (2.19) such that $\dot{\epsilon}_{ij}^{\mathrm{pc}}$ will not be identically zero, but sufficiently close to zero. Numerically, the determination of the penalty parameter E_0 is based on a convergence study. A parametric study on E_0 has been performed where $\epsilon_{ij}^{\mathrm{pc}} = \int \dot{\epsilon}_{ij}^{\mathrm{pc}} \mathrm{d}t$ and $q_{ij}^{\mathrm{c}} = \int \dot{q}_{ij}^{\mathrm{c}} \mathrm{d}t$ have been calculated. The parameter E_0 has successively been increased until q_{ij}^{c} has converged to a saturated value, which has been observed at $E_0 = 100H$. It should be noted that if too large values of E_0 is used, large numerical error may be introduced.

When using additional degrees of freedom in the plastic regime only, the issue of elastic-plastic transition and loading-unloading requires special attention. This means activating or deactivating of degrees of freedom depending on if a point is considered as elastic or plastic. As an alternative to a rate-independent formulation, a rate-dependent formulation with a large rate-sensitivity exponent can be used, see e.g. Gudmundson (2004). Then, the elastic-plastic boundary is smeared out and all points are considered equally. Additional degrees of freedom also necessitate careful consideration of boundary conditions. When using a commercial finite element code as in the present implementation, a wide range of other elements are available which potentially could be used in an analysis together with the higher-order element. At the boundaries between two different types of elements, all degrees of freedom that share the nodes at the boundary will obtain the same value due to continuity. In the present

context, the same situation is found at an elastic-plastic boundary where the plastic strain has to vanish in the plastic material at the boundary to the elastic material. If the higher-order boundary condition on plastic strain is to be removed, the corresponding degrees of freedom have to be unconstrained. This can be achieved either if an extra node set is used at the boundary, at which only the displacement degrees of freedom are coupled, or if two different types of elements are used, where plastic strain does not exist in one of the elements.

5 Conclusions

In contrast to the situation ten years ago, there is today a large body of work done on modelling with gradient theories of plasticity. It seems that only during the last couple of years, the theories converge to a more or less common framework. We here use the framework of higher-order strain gradient plasticity laid down by Gudmundson (2004) accompanied by a complete set of FE-equations. The gradient effects, which are the origin for the ability of capturing the size-dependence, are introduced in the free energy only. The dissipation is not affected by plastic strain gradients, and hence we call the conjugate stresses energetic. A penalty parameter is here used for simplicity in order to fulfill the consistency relation. Finite element equations are presented for a general 3D implementation and is in the present work applied in a 2D analysis. The theory uses the plastic strain tensor as additional dof in addition to the displacements. Plastic incompressibility is used to reduce the number of unknown plastic strains from six to five, which leads to a maximum of eight dof per node. Resulting differential equations are of second order both for displacements and plastic strains and consequently only C_0-continuity of the elements has to be fulfilled. A number of element types has been tested and the **4F** and **8CR** elements are recommended in the present analysis.

Finally, the theoretical framework is applied in a finite element analysis of an idealized plane strain cell model of a metal matrix composite subjected to pure shear loading. We claim that the present MMC model has a high physical relevance for polycrystals with random grain orientation. A comparison with the work by Bittencourt et al. (2003) has been done and both differences and similarities can be concluded. The present isotropic formulation cannot capture differences in behaviour for MMCs with different fiber shape but the same volume fraction. Size effects that are controlled by the fiber size at constant fiber volume fraction can be captured with the present theory but not with standard plasticity theory.

A closed form solution to pure shear of a thin film is presented and it is concluded that the functional form of the solution coincides with the corre-

sponding solution by Gurtin (2002).

Acknowledgements

Per Fredriksson and Peter Gudmundson gratefully acknowledge the financial support from the Swedish Research Council under contract 621-2001-2643.

Appendix A – Matrix formulation of finite element equations

The purpose of this section is to describe the matrix formulation which is the basis for Eq. (2.32). The derivation is intended for 3D elements but will be used in 2D plane strain analysis. The theory utilizes node displacements d_i and node plastic strains e_{ij} as dof. Within one element, the displacement field $\mathbf{u}_{\mathrm{u}}^{\mathrm{T}} = \left[u_1 \; u_2 \; u_3 \right]$ are interpolated as

$$\mathbf{u}_{\mathrm{u}} = \mathbf{N}_{\mathrm{u}} \mathbf{d} \tag{A-1}$$

where

$$\mathbf{N}_{\mathrm{u}} = \left[\mathbf{N}_{\mathrm{u}}^1 \; \mathbf{N}_{\mathrm{u}}^2 \quad \cdots \; \mathbf{N}_{\mathrm{u}}^{n_{\mathrm{u}}} \right] \tag{A-2}$$

$$\mathbf{N}_{\mathrm{u}}^I = \mathrm{diag} \left[N_{\mathrm{u}}^I \; N_{\mathrm{u}}^I \; N_{\mathrm{u}}^I \right] \tag{A-3}$$

$$\mathbf{d}^{\mathrm{T}} = \left[d_1^1 \; d_2^1 \; d_3^1 \; d_1^2 \; d_2^2 \; d_3^2 \quad \cdots \; d_1^{n_{\mathrm{u}}} \; d_2^{n_{\mathrm{u}}} \; d_3^{n_{\mathrm{u}}} \right] \tag{A-4}$$

and n_{u} is the number of nodes used for the interpolation of u_i. N_{u}^I are shape functions and the vector $\mathbf{d}$ contains $3n_{\mathrm{u}}$ nodal dof for a 3D element.

The plastic strain field $(\boldsymbol{\epsilon}^{\mathrm{p}})^{\mathrm{T}} = \left[\epsilon_{11}^{\mathrm{p}} \; \epsilon_{22}^{\mathrm{p}} \; \epsilon_{33}^{\mathrm{p}} \; \gamma_{12}^{\mathrm{p}} \; \gamma_{13}^{\mathrm{p}} \; \gamma_{23}^{\mathrm{p}} \right]$ requires more special treatment. Since plastic deformation is assumed to be incompressible, the six components of the plastic strain tensor can be reduced to five. We have chosen $\epsilon_{33}^{\mathrm{p}}$ as the dependent variable, which means that for variables of node I, the following transformation can be used

$$\begin{bmatrix} e^I_{11} \\ e^I_{22} \\ e^I_{33} \\ e^I_{12} \\ e^I_{13} \\ e^I_{23} \end{bmatrix} = \begin{bmatrix} 1 & 0\,0\,0\,0 \\ 0 & 1\,0\,0\,0 \\ -1 & -1\,0\,0\,0 \\ 0 & 0\,1\,0\,0 \\ 0 & 0\,0\,1\,0 \\ 0 & 0\,0\,0\,1 \end{bmatrix} \begin{bmatrix} e^I_{11} \\ e^I_{22} \\ e^I_{12} \\ e^I_{13} \\ e^I_{23} \end{bmatrix} = \mathbf{C}\mathbf{e} \tag{A-5}$$

The formulation takes the following form

$$\boldsymbol{\epsilon}^{\mathrm{p}} = \mathbf{N}_{\mathrm{p}}\mathbf{e} \tag{A-6}$$

where

$$\mathbf{N}_{\mathrm{p}} = \begin{bmatrix} \mathbf{N}^1_{\mathrm{p}}\mathbf{C} & \mathbf{N}^2_{\mathrm{p}}\mathbf{C} & \cdots & \mathbf{N}^{n_{\mathrm{p}}}_{\mathrm{p}}\mathbf{C} \end{bmatrix} \tag{A-7}$$

$$\mathbf{N}^I_{\mathrm{p}} = \mathrm{diag}\begin{bmatrix} N^I_{\mathrm{p}} & N^I_{\mathrm{p}} & N^I_{\mathrm{p}} & N^I_{\mathrm{p}} & N^I_{\mathrm{p}} & N^I_{\mathrm{p}} \end{bmatrix} \tag{A-8}$$

$$\mathbf{e}^{\mathrm{T}} = \begin{bmatrix} e^1_{11} & e^1_{22} & e^1_{12} & e^1_{13} & e^1_{23} & \cdots & e^{n_{\mathrm{p}}}_{13} & e^{n_{\mathrm{p}}}_{23} \end{bmatrix} \tag{A-9}$$

and where $\mathbf{e}$ is a vector with $5n_{\mathrm{p}}$ nodal dof at n_{p} nodes.

Strains and plastic strain gradients are obtained as derivatives of the variables $\mathbf{u}_{\mathrm{u}}$ and $\boldsymbol{\epsilon}^{\mathrm{p}}$, respectively. For the strains, the conventional approach is adopted

$$\begin{bmatrix} \epsilon_{11} \\ \epsilon_{22} \\ \epsilon_{33} \\ \gamma_{12} \\ \gamma_{13} \\ \gamma_{23} \end{bmatrix} = \begin{bmatrix} \sum_{I=1}^{n_{\mathrm{u}}} B^I_{\mathrm{u}1} d^I_1 \\ \sum_{I=1}^{n_{\mathrm{u}}} B^I_{\mathrm{u}2} d^I_2 \\ \sum_{I=1}^{n_{\mathrm{u}}} B^I_{\mathrm{u}3} d^I_3 \\ \sum_{I=1}^{n_{\mathrm{u}}} \left(B^I_{\mathrm{u}1} d^I_2 + B^I_{\mathrm{u}2} d^I_1 \right) \\ \sum_{I=1}^{n_{\mathrm{u}}} \left(B^I_{\mathrm{u}1} d^I_3 + B^I_{\mathrm{u}3} d^I_1 \right) \\ \sum_{I=1}^{n_{\mathrm{u}}} \left(B^I_{\mathrm{u}2} d^I_3 + B^I_{\mathrm{u}3} d^I_2 \right) \end{bmatrix} = \mathbf{B}_{\mathbf{u}}\mathbf{d} \tag{A-10}$$

We also have

$$\mathbf{B}_{\mathrm{u}} = \left[\begin{array}{cccc} \mathbf{B}_{\mathrm{u}}^{1} & \mathbf{B}_{\mathrm{u}}^{2} & \cdots & \mathbf{B}_{\mathrm{u}}^{n_{\mathrm{u}}} \end{array} \right] \tag{A-11}$$

$$\mathbf{B}_{\mathrm{u}}^{I} = \left[\begin{array}{ccc} B_{\mathrm{u}1}^{I} & 0 & 0 \\ 0 & B_{\mathrm{u}2}^{I} & 0 \\ 0 & 0 & B_{\mathrm{u}3}^{I} \\ B_{\mathrm{u}2}^{I} & B_{\mathrm{u}1}^{I} & 0 \\ B_{\mathrm{u}3}^{I} & 0 & B_{\mathrm{u}1}^{I} \\ 0 & B_{\mathrm{u}3}^{I} & B_{\mathrm{u}2}^{I} \end{array} \right] \tag{A-12}$$

where $B_{\mathrm{u}k}^{I} = \frac{\partial N_{\mathrm{u}}^{I}(\xi_j)}{\partial x_k}$ involves the Jacobian for the geometrical mapping for node I. Plastic strain gradients are obtained on the same arguments as for the plastic strains as

$$\left[\begin{array}{c} \epsilon_{11,1}^{\mathrm{p}} \\ \epsilon_{22,1}^{\mathrm{p}} \\ \epsilon_{33,1}^{\mathrm{p}} \\ \gamma_{12,1}^{\mathrm{p}} \\ \vdots \\ \epsilon_{33,3}^{\mathrm{p}} \\ \gamma_{12,3}^{\mathrm{p}} \\ \gamma_{13,3}^{\mathrm{p}} \\ \gamma_{23,3}^{\mathrm{p}} \end{array} \right] = \left[\begin{array}{c} \sum_{I=1}^{n_{\mathrm{p}}} B_{\mathrm{p}1}^{I} e_{11}^{I} \\ \sum_{I=1}^{n_{\mathrm{p}}} B_{\mathrm{p}1}^{I} e_{22}^{I} \\ \sum_{I=1}^{n_{\mathrm{p}}} \left(-B_{\mathrm{p}1}^{I} e_{11}^{I} - B_{\mathrm{p}1}^{I} e_{22}^{I} \right) \\ \sum_{I=1}^{n_{\mathrm{p}}} B_{\mathrm{p}1}^{I} e_{12}^{I} \\ \vdots \\ \sum_{I=1}^{n_{\mathrm{p}}} \left(-B_{\mathrm{p}3}^{I} e_{11}^{I} - B_{\mathrm{p}3}^{I} e_{22}^{I} \right) \\ \sum_{I=1}^{n_{\mathrm{p}}} B_{\mathrm{p}3}^{I} e_{12}^{I} \\ \sum_{I=1}^{n_{\mathrm{p}}} B_{\mathrm{p}3}^{I} e_{13}^{I} \\ \sum_{I=1}^{n_{\mathrm{p}}} B_{\mathrm{p}3}^{I} e_{23}^{I} \end{array} \right] = \mathbf{B}_{\mathrm{p}} \mathbf{e} \tag{A-13}$$

where

$$\mathbf{B}_{\mathrm{p}} = \left[\begin{array}{cccc} \mathbf{B}_{\mathrm{p}1}^{1}\mathbf{C} & \mathbf{B}_{\mathrm{p}1}^{2}\mathbf{C} & \cdots & \mathbf{B}_{\mathrm{p}1}^{n_{\mathrm{p}}}\mathbf{C} \\ \mathbf{B}_{\mathrm{p}2}^{1}\mathbf{C} & \mathbf{B}_{\mathrm{p}2}^{2}\mathbf{C} & \cdots & \mathbf{B}_{\mathrm{p}2}^{n_{\mathrm{p}}}\mathbf{C} \\ \mathbf{B}_{\mathrm{p}3}^{1}\mathbf{C} & \mathbf{B}_{\mathrm{p}3}^{2}\mathbf{C} & \cdots & \mathbf{B}_{\mathrm{p}3}^{n_{\mathrm{p}}}\mathbf{C} \end{array} \right] \tag{A-14}$$

$$\mathbf{B}_{\mathrm{p}j}^{I} = \mathrm{diag} \left[\begin{array}{cccccc} B_{\mathrm{p}j}^{I} & B_{\mathrm{p}j}^{I} & B_{\mathrm{p}j}^{I} & B_{\mathrm{p}j}^{I} & B_{\mathrm{p}j}^{I} & B_{\mathrm{p}j}^{I} \end{array} \right] \tag{A-15}$$

where $B_{\mathrm{u}k}^{I} = \frac{\partial N_{\mathrm{p}}^{I}(\xi_j)}{\partial x_k}$ and $\mathbf{C}$ is defined above .

The Cauchy stress, micro stress and moment stress vectors are introduced as

$$\mathbf{s}_{\mathrm{u}}^{\mathrm{T}} = \begin{bmatrix} \sigma_{xx} & \sigma_{yy} & \sigma_{zz} & \tau_{xy} & \tau_{xz} & \tau_{yz} \end{bmatrix} \tag{A-16}$$

$$\mathbf{q}^{\mathrm{T}} = \begin{bmatrix} q_{xx} & q_{yy} & q_{zz} & q_{xy} & q_{xz} & q_{yz} \end{bmatrix} \tag{A-17}$$

$$\mathbf{m}^{\mathrm{T}} = \begin{bmatrix} m_{xxx} & m_{yyx} & m_{zzx} & m_{xyx} & m_{xzx} & m_{yzx} & \cdots & m_{xzz} & m_{yzz} \end{bmatrix} \tag{A-18}$$

and the conventional and higher-order traction vectors as

$$\mathbf{t}_{\mathrm{u}} = \begin{bmatrix} \sigma_{xx}n_x + \sigma_{xy}n_y + \sigma_{xz}n_z \\ \sigma_{xy}n_x + \sigma_{yy}n_y + \sigma_{yz}n_z \\ \sigma_{xz}n_x + \sigma_{yz}n_y + \sigma_{zz}n_z \end{bmatrix} \tag{A-19}$$

$$\mathbf{t}_{\mathrm{p}} = \begin{bmatrix} m_{xxx}n_x + m_{xxy}n_y + m_{xxz}n_z \\ m_{yyx}n_x + m_{yyy}n_y + m_{yyz}n_z \\ m_{zzx}n_x + m_{zzy}n_y + m_{zzz}n_z \\ m_{xyx}n_x + m_{xyy}n_y + m_{xyz}n_z \\ m_{xzx}n_x + m_{xzy}n_y + m_{xzz}n_z \\ m_{yzx}n_x + m_{yzy}n_y + m_{yzz}n_z \end{bmatrix} \tag{A-20}$$

A collective matrix formulation for both sets of discretized variables, i.e. displacement and plastic strain will now be presented. For every element, the vectors $\mathbf{u}^{\mathrm{T}} = \begin{bmatrix} (\mathbf{u}_{\mathrm{u}})^{\mathrm{T}} & (\boldsymbol{\epsilon}^{\mathrm{p}})^{\mathrm{T}} \end{bmatrix}$ and $(\mathbf{u}')^{\mathrm{T}} = \begin{bmatrix} (\boldsymbol{\epsilon})^{\mathrm{T}} & (\boldsymbol{\epsilon}^{\mathrm{p}})^{\mathrm{T}} & (\boldsymbol{\epsilon}^{\mathrm{p}'})^{\mathrm{T}} \end{bmatrix}$ are introduced, where $\boldsymbol{\epsilon}^{\mathrm{p}'}$ is a vector of plastic strain gradients, such that

$$\mathbf{u} = \mathbf{N}\mathbf{p} \tag{A-21}$$

$$\mathbf{u}' = \mathbf{B}\mathbf{p} \tag{A-22}$$

where

$$\mathbf{N} = \begin{bmatrix} \mathbf{N}_{\mathrm{u}} & \mathbf{0} \\ \mathbf{0} & \mathbf{N}_{\mathrm{p}} \end{bmatrix}, \quad \mathbf{B} = \begin{bmatrix} \mathbf{B}_{\mathrm{u}} & \mathbf{0} \\ \mathbf{0} & \mathbf{N}_{\mathrm{p}} \\ \mathbf{0} & \mathbf{B}_{\mathrm{p}} \end{bmatrix}, \quad \mathbf{p} = \begin{bmatrix} \mathbf{d} \\ \mathbf{e} \end{bmatrix} \tag{A-23}$$

and $\mathbf{0}$ is the zero matrix. We introduce the vectors

$$\mathbf{s} = \begin{bmatrix} \mathbf{s}_\mathrm{u} \\ \mathbf{q} - \mathbf{s}_\mathrm{u} \\ \mathbf{m} \end{bmatrix}, \quad \mathbf{t} = \begin{bmatrix} \mathbf{t}_\mathrm{u} \\ \mathbf{t}_\mathrm{p} \end{bmatrix} \tag{A-24}$$

for the stresses. If all of the above is inserted in the variational principle Eq. (2.25) and utilizing that the variations $\delta\mathbf{u}$ and $\delta\mathbf{p}$ are arbitrary, the following equation is obtained

$$\mathbf{k}_\mathrm{e}\dot{\mathbf{p}}^{n+1} = \dot{\mathbf{f}}_\mathrm{e}^{n+1} - \{\mathbf{c}_\mathrm{i}^n - \mathbf{c}_\mathrm{e}^n\} \tag{A-25}$$

The bracket terms are equilibrium correction terms evaluated at $t = t_n$, which explicitly read

$$\mathbf{c}_\mathrm{i} = \int_S \mathbf{B}^\mathrm{T}\mathbf{s}\mathrm{d}V, \quad \mathbf{c}_\mathrm{e} = \int_S \mathbf{N}^\mathrm{T}\mathbf{t}\mathrm{d}S \tag{A-26}$$

References

Abaqus/Standard 6.7, 2006. Abaqus Users' Manual. (www.simulia.com).

Aifantis, E. C., 1987. The physics of plastic deformation. Int J Plast 3, 211–247.

Aifantis, K. E., Willis, J. R., 2005. The role of interfaces in enhancing the yield strength of composites and polycrystals. J Mech Phys Solids 53, 1047–1070.

Anand, L., Gurtin, M. E., Lele, S. P., Gething, C., 2005. A one-dimensional theory of strain gradient plasticity: Formulation, analysis, numerical results. J Mech Phys Solids 53, 1789–1826.

Bassani, J. L., Needleman, A., Van der Giessen, E., 2001. Plastic flow in a composite: a comparison of nonlocal continuum and discrete dislocation predictions. Int J Solids Struct 38, 833–853.

Bittencourt, E., Needleman, A., Gurtin, M. E., Van der Giessen, E., 2003. A comparison of nonlocal continuum and discrete dislocation plasticity predictions. J Mech Phys Solids 51, 281–310.

Borg, U., Fleck, N. A., 2007. Strain gradient effects in surface roughening. Mod Simul Mat Sci Eng 15, 1–12.

Borg, U., Kysar, J. W., 2007. Strain gradient crystal plasticity analysis of a single crystal containing a cylindrical void. Int J Solids Struct 44, 6382–6397.

Cermelli, P., Gurtin, M. E., 2002. Geometrically necessary dislocations in viscoplastic single crystals and bicrystals undergoing small deformations. Int J Solids Struct 39, 6281–6309.

Cleveringa, H. H. M., Van der Giessen, E., Needleman, A., 1997. Comparison of discrete dislocation and continuum plasticity predictions for a composite material. Acta Mater 45, 3163–3179.

de Borst, R., Mühlhaus, H. B., 1992. Gradient-dependent plasticity: formulation and algorithmic aspects. Int J Num Meth Eng 35, 521–539.

de Borst, R., Pamin, J., 1996. Some novel developments in finite element procedures for gradient-dependent plasticity. Int J Num Meth Eng 39, 2477–2505.

Fleck, N. A., Hutchinson, J. W., 1997. Strain gradient plasticity. Adv Appl Mech 33, 295–361.

Fleck, N. A., Hutchinson, J. W., 2001. A reformulation of strain gradient plasticity. J Mech Phys Solids 49, 2245–2271.

Fleck, N. A., Willis, J. R., 2004. Bounds and estimates for the effect of strain gradients upon the effective plastic properties of an isotropic two-phase composite. J Mech Phys Solids 52, 1855–1888.

Fredriksson, P., Gudmundson, P., 2007. Modelling of the interface between a thin film and a substrate within a strain gradient plasticity framework. J Mech Phys Solids 55, 939–955.

Fredriksson, P., Larsson, P.-L., 2008. Wedge indentation of thin films modelled by strain gradient plasticity. Int J Solids Struct 45, 5556–5566.

Gudmundson, P., 2004. A unified treatment of strain gradient plasticity. J Mech Phys Solids 52, 1379–1406.

Gudmundson, P., Fredriksson, P., 2003. Thickness dependence of viscoplastic deformations in thin films. In: 9th international conference on the mechanical behaviour of materials, ICM9, Geneva.

Gurtin, M. E., 2002. A gradient theory of single-crystal viscoplasticity that accounts for geometrically necessary dislocations. J Mech Phys Solids 50, 5–32.

Lloyd, D. J., 1994. Particle reinforced aluminium and magnesium matrix composites. Int Mat Rev 39, 1–23.

Mikkelsen, L. P., 1997. Post-necking behaviour modelled by a gradient dependent plasticity theory. Int J Solids Struct 34, 4531–4546.

Mikkelsen, L. P., 2007. Implementing a gradient dependent plasticity model in abaqus. In: 2007 Abaqus Users' Conference, SIMULIA, Paris, France. pp. 482–492.

Niordson, C. F., Hutchinson, J. W., 2003. Non-uniform plastic deformation of micron scale objects. Int J Num Meth Eng 56, 961–975.